Chin. J. Astron. Astrophys. Vol. 1, No. 6, (2001) 507–513
(http://www.chjaa.org or http://chjaa.bao.ac.cn)

Chinese Journal of
Astronomy and
Astrophysics

Multi-frequency VLBI Observations of NRAO 150

Yong-Jun Chen ⋆, Dong-Rong Jiang and Fu-Jun Zhang

Shanghai Astronomical Observatory, Chinese Academy of Sciences, Shanghai 200030
National Astronomical Observatories, Chinese Academy of Sciences, Beijing 100012

Received 2001 June 8; accepted 2001 September 3

Abstract We present multi-frequency, high resolution, radio structures of NRAO 150 with VLBA and EVN array respectively, both of which show a very collimated one-sided jet structure beyond an angular distance of 80 mas. Model fitting is performed for observations at 2.3 GHz and 8.4 GHz which reveal the source to be consisting of several components at position angle $\sim 30°$. According to the light curves at 4.8 GHz, 8.0 GHz and 14.5 GHz an outburst is currently occurring in its rising stage, which suggests that a new component is probably in the course of forming. Spectral analysis reveals that the new component probably has a higher spectral index. The maximum proper motion of ~ 0.46 mas yr^{-1} is expected if we suppose that the new component is moving away from core at the beginning of the flaring.

Key words: galaxies: active – galaxies: radio source: individual: NRAO 150 – radio structure: galaxies

1 INTRODUCTION

NRAO 150 is one among the strongest and most variable extragalactic sources at centimeter wavelengths (Phillips & Shaffer 1983). NRAO 150 has at least four major compact components, ranging in size from less than 1 mas to 25 mas or more, as well as extended structure indicated by low frequency emission. At 10.65 GHz and 22.7 GHz, NRAO 150 has been modelled as a close double, with a separation of about 0.6 mas and individual components as small as 0.2 mas (Kellermann et al. 1977). Limited by the relatively low sensitivity of antennas and technique level at the time, some structures were not recovered very well. In our present paper, we present somewhat different radio structures, which show a typical core-jet radio structure at three different frequencies. In addition, it has been argued that this very compact source is embedded in the brightest part of a very different, complex source seen in 1.67 GHz maps (Mutel & Phillips 1980).

Being a low Galactic latitude object, NRAO 150 was optically unidentified (Phillips & Shaffer 1983). No detections in optical, X-ray or γ-ray bands have ever been reported in any publications, and we know little about the source. We also do not know the redshift of the

⋆ E-mail: cyj@center.shao.ac.cn

source for the same reasons. However, infrared emissions were detected with a spectral index of ~ -1.5 ($F_\nu \propto \nu^\alpha$) in 1983 by Roellig (1986). We are not sure whether the value is true or not, because since then no more infrared data has been published.

Since no optical counterpart is identified as of date, the principal way for deep research into the radio source can only be through observation at radio and far infrared bands. In Section 2, we describe observations of NRAO 150 at 2.3 GHz 5 GHz and 8.4 GHz, where the specific process is given for the observation at 5 GHz, and the observational results are given in Section 3. Finally we present a discussion in Section 4.

2 OBSERVATIONS

VLBI observations at 2.3 GHz and 8.4 GHz were made with the VLBA for geodetic and astrometric purposes. These observations are made in a bandwidth synthesis mode at standard frequencies of 2.3 GHz (S band) and 8.4 GHz (X band). Dual-frequency observations allow for an accurate calibration of the frequency-dependent propagation delay introduced by the ionosphere, so we can have high quality data for imaging (Ma et al. 1998). We got visibility data and images at 2.3 Ghz and 8.4 GHz from The Radio Reference Frame Image Database, and then re-imaged for further analysis.

Observation at 5 GHz was performed with a 10-station VLBI array on Feb. 18, 1997, from UT $10^{\rm h}0^{\rm m}$ to $22^{\rm h}0^{\rm m}$. The array consisted of the telescopes at Sheshan, Urumqi, Effelsberg, Medicina, Noto, Onsala, Westbork, Turun, HartRAO and Jodrell Bank. Of these Noto failed to make the observation; Urumqi and Jodrell Bank recorded in the wrong polarization. Thus we had effective data from seven stations. The maximum baseline length in both the north-south and ease-west directions was $\sim$ 120 million wavelengths (corresponding to an angular resolution of $\sim$ 1 mas). Because of the abortive observation of three telescopes, the (u, v) coverage of the observation was considerably reduced, especially in the region between the short and long baselines, due to lack of sampling. This should have some impact on our hybrid map and model fitting, and some details of its radio structure might have been lost.

Amplitude calibration for each antenna is derived from measurements of the antenna gain and system temperatures. Global fringe fitting is performed using the AIPS task FRING, an implementation of the Schwab & Cotton (1983) algorithm. The fringe fitting is performed on each IF independently using a solution interval of 2 minutes, and a point source model is assumed. After completing the data processing initiation, an interval of 45 seconds is used to average the data so as to improve the signal-to-noise ratio. Since the source structure is relatively small, the imaging field is slightly affected by the averaging effect. The specific imaging process of the visibility data at the three frequencies is made within difmap and CLEAN and SELF-CALIBRATION are alternately used during the processing. Finally, model fitting are performed for the 2.3 GHz and 8.4 GHz VLBI visibility data. We obtained satisfactory results, which are in good agreement with the radio structure given by hybrid imaging. For the observation at 5 GHz, it was difficult for us to make the model converge to a unique solution during the model fitting due to the poor (u, v) coverage.

3 RESULTS

Figure 1 shows the radio structure of NRAO 150 at 2.3 GHz, in which the top map shows the hybrid map, and the bottom map gives the result of model fitting. In this map NRAO 150

presents a typical core-jet radio structure at position angle $\sim 30°$; the noise level is ~ 1.05 mJy /beam. The jet structure is composed of several components on a scale of ~ 80 mas, which suggests that the radio structure is highly collimated at least on this scale. Model fitting to the visibility data reveals that with five Gaussian components, an optimum result can be obtained. The detailed parameters for each component are listed in Table 1. Comparison is made between the hybrid map and model-fitting map, which reveals that the peak intensities for the two maps are very close, and the noise levels are also very near to each other, and that, most importantly, the radio structures are almost completely alike. These imply that the visibility data are of higher quality, and that, more importantly, the resultant images are reliable.

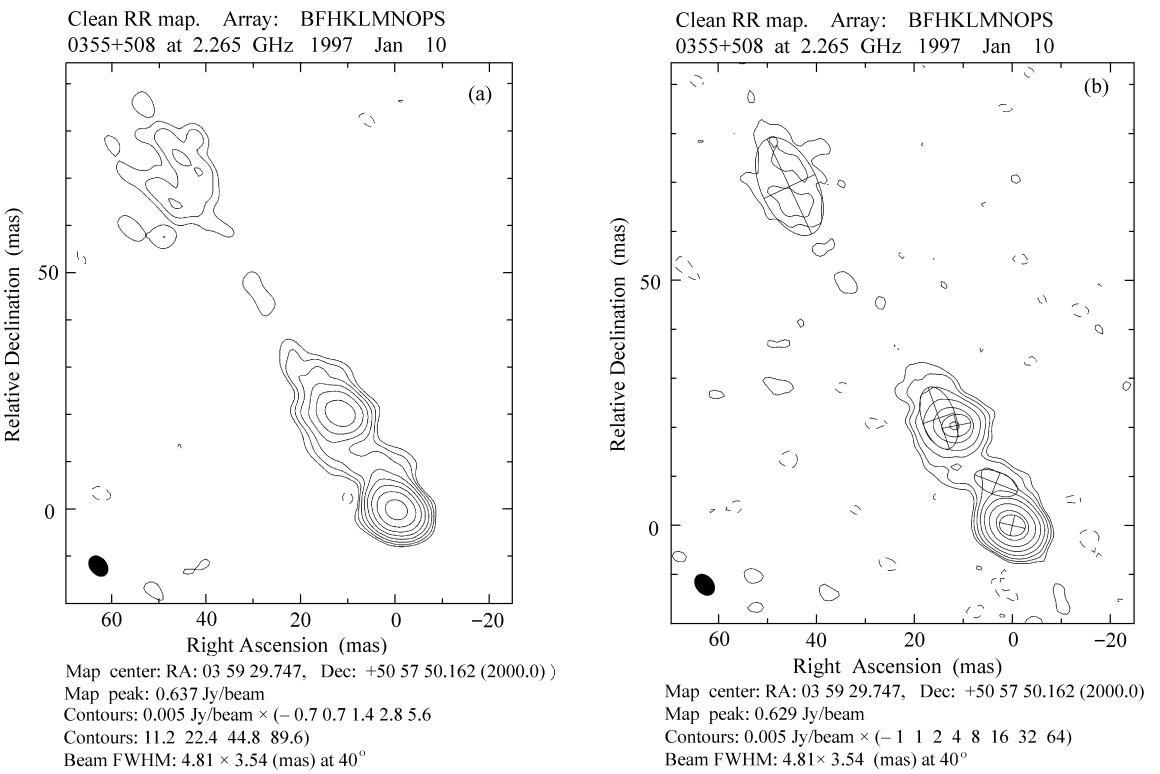

Fig. 1 Radio structure of NRAO 150 at 2.3 GHz. (a) Hybrid map; (b) Image of model fitting.

Table 1 Model Fitting Parameters of Radio Structure of NRAO 150

Comp.	VLBI Observation at 8.4 GHz			Comp.	VLBI Observation at 8.4 GHz		
	Flux (Jy)	Radius (mas)	Theta (deg)		Flux (Jy)	Radius (mas)	Theta (deg)
C_0	1.487	0.00	0.00	D_0	1.285	0.00	0.00
C_1	0.096	9.26	21.11	D_1	0.195	1.91	48.30
C_2	0.381	23.37	29.30	D_2	0.037	4.48	38.94
C_3	0.241	26.56	34.40	D_3	0.064	24.23	31.41
C_4	0.168	82.81	33.34				

A much higher resolution radio structure by a factor of ~ 3 is given in the top map of Figure 2 in comparison with the Figure 1 due to the higher observing frequency of 8.4 GHz. They belong to the same project, having equally high quality of visibility. The participated telescopes are also the same. It is therefore natural that a high quality result is expected. The noise level is ~ 0.94 mJy/beam, and the position angle is approximately 30 degree also. Through model fitting we obtained a good simulation to visibility data with an analogous radio structure, and very near the same peak intensity and noise level as the hybrid map. The specific parameters of Gaussian model component are also listed in Table 1, in which the outermost component presented in Figure 1 is absent on account of the much smaller clean beam.

EVN observation at 5 GHz was performed about one month later. Due to lack of three telescopes, and more importantly because NRAO 150 was observed merely as a calibrator in the project, very limited number of scans were assigned to the object so that the (u, v) coverage was poor. We can surely expect the hybrid image not as good as what we have got from the VLBA observation. Here we just present the cleaned map in Figure 3 with position angle of $\sim 30^\circ$ and noise level of ~ 2.58 mJy/beam; it shows a similar radio structure to the 8.4 GHz observational result. The lowest contour level is two times worse and the dynamical range is even worse still in comparison with the structure found at 8.4 GHz, even though they have similar resolutions. Model fitting is also performed but we cannot obtain a convergent solution due to the poor (u, v) coverage.

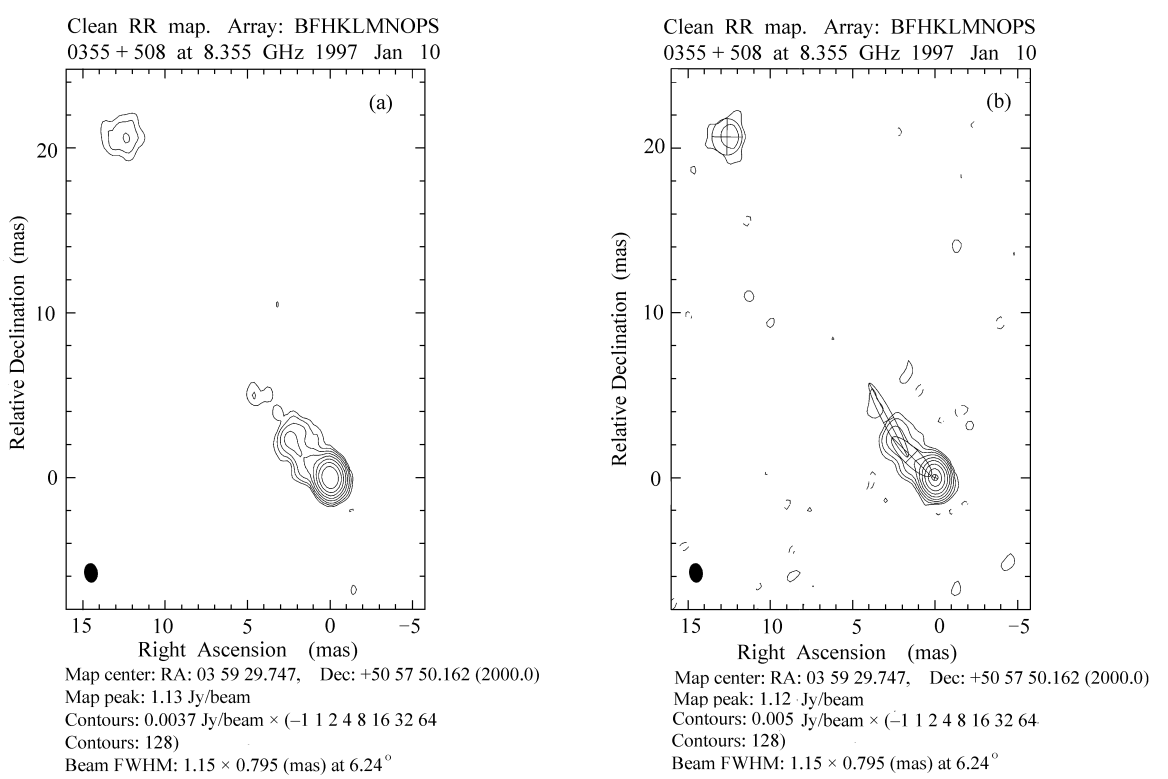

Fig. 2 Radio structure of NRAO 150 at 8.4 GHz. (a) Hybrid map; (b) Image of model fitting.

Since radio flux density varies fairly slowly, the VLBI observation dates at the three frequencies can be thought to be almost simultaneous. Comparisons among the structures at these three different frequencies will be useful in probing the physical radio structure and its properties. Suppose that the radio flux comes from progressively larger regions (than the optical flux) as the radio frequency decreases, then component C_0 in Figure 1 basically corresponds to the combination of components D_0, D_1 and D_2 in Figure 2. Due to the much lower resolution of observation at 2.3 GHz; components C_1, C_2 and C_4 have no corresponding components in Figure 2 because they are too weak at that resolution to be observed. Component C_3 corresponds to component D_3, if there is a one-to-one correspondence between the component at the two frequencies. We also compared the observational results at 5 GHz and 8.4 GHz. Since both observations have a very similar resolution, we suggest pretty positively that components D_0, D_2 and D_3 at 8.4 GHz have corresponding components at 5.0 GHz while component D_1 has no corresponding component in Figure 3 because the latter has too low a sensitivity.

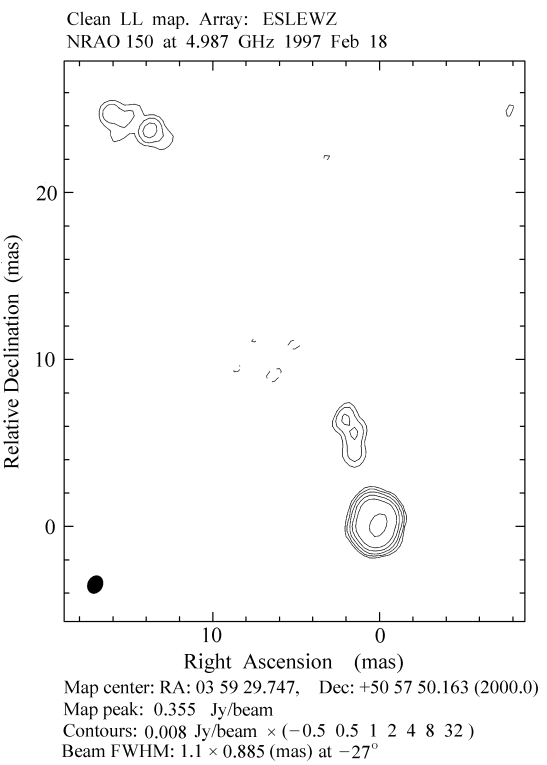

Fig. 3 Radio structure of NRAO 150 at 5 GHz.

Although the VLBI observations at three different frequencies were carried out on close together dates, unfortunately the observation at 2.3 GHz had a much lower resolution than that at the other two frequencies, and the sensitivity for the EVN observation is much lower. This makes it impossible to do spectral analysis of each component or to get more information on the jet structure of the source.

4 DISCUSSION

As mentioned above, no emission at optical or higher frequency wave bands has ever been detected. The study on the source is mainly confined in the radio region. Due to the fact that NRAO 150 is a compact and strong radio source, the source has been being monitored nearly over the whole of the last three decades at 5 GHz, 8 GHz and 14.5 GHz by the 26-meter telescope of the University of Michigan Radio Astronomy Observatory (UMRAO). The light curves at these bands are shown in Figure 4. It is clear from the map that an outburst started approximately in 1993, which is now still in its rising stage. This might imply that a new component in the image of high resolution structure should be observed if the observational resolution and sensitivity are both high enough (Chu et al. 1996) . We inspect these images and find that the nearest component to core is the component D_1 in Figure 2, which is ~ 1.91 mas away from the core. The corresponding component is not found in Figure 3 probably due to

the much lower sensitivity in comparison with the observation at 8.4 GHz (see the previous section);—it was reasonable to make such a comparison at all because they have a similar size of clean beam. However we find in Table 1 that component D_1 has a higher flux than component D_2. A natural guess would be that a component in Figure 3 corresponding to component D_1 not D_2 should be detected at 5 GHz, yet this is not the case, where it is the weaker component instead that has a corresponding component in Figure 3. The difference in frequency is probably the main reason for this unexpected feature. A similar situation is also shown in Figure 1 and Figure 2: the stronger component C_2 has no corresponding component, but the nearby, weaker component C_3 has one if we believe that the radio flux of decreasing frequency comes from progressively larger regions (than the optical flux). Therefore it is clear that the new component is either component D_1 or is another component overwhelmed by nuclear emission. This new component will have a fairly high spectral index which is shown in Figure 5, in which the spectral index shows small fluctuations before 1993, and began to rise since. Unfortunately we cannot identify the new component through spectral index for each component due to the different resolutions and/or sensitivities.

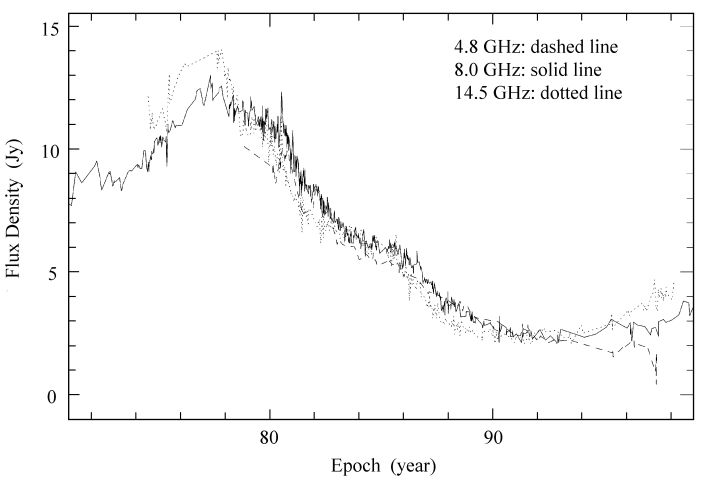

Fig. 4 Light curves at 5 GHz, 8 GHz and 14.5 GHz of NRAO 150.

NRAO 150 is one of the smallest, very strong radio sources with flat spectrum at radio frequency (see Figure 5). Most of the flux density at 7.85 GHz emanates from a region ~ 1 ms in diameter (Bääth et al. 1980). From observations at 5 GHz (Kellermann et al. 1971) it was found that most of the flux density comes from a region 1.3 mas in diameter. At lower frequencies, the source appears to be somewhat larger: at 1.66 GHz more than 70% of the flux density emanates from a region of diameter ~ 8 mas (Shaffer & Schilizzi 1975). Similar situations also appear in the VLBI observations at 2.3 GHz and 8.4 GHz in our present case. In addition, no two-sided jet structure of the source has ever been detected in any high resolution observation to date. All these can easily make us associate it with superluminal radio sources. Suppose that the new component originates from the core at a time when the total flux density is minimum in the light curves, then we can derive a maximum proper motion of ~ 0.46 mas yr^{-1} using the component D_1. Unfortunately we have no information on redshift and observational data at high frequency of the source, otherwise we can get more information on the apparent

velocity to determine whether or not NRAO 150 is a superluminal radio source and the beaming effect operates.

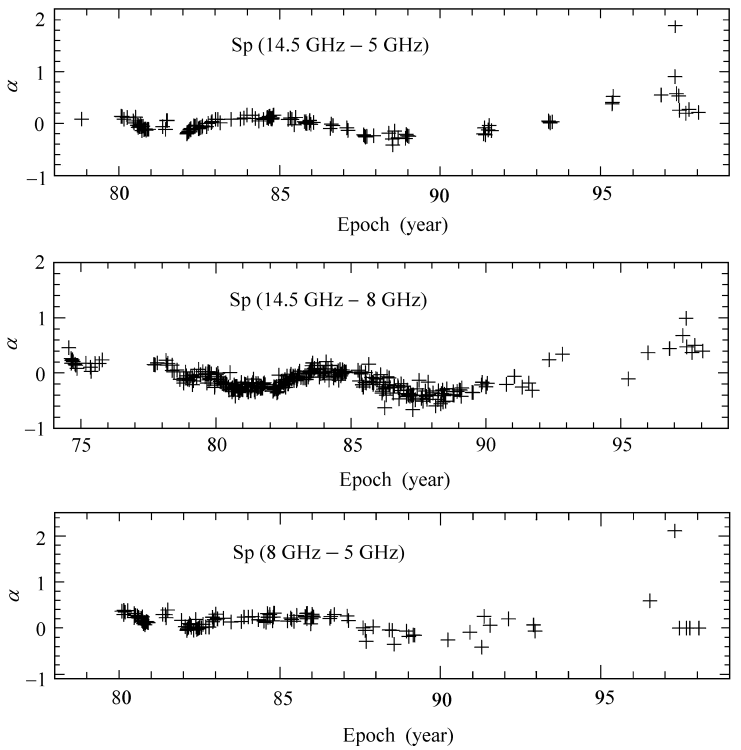

Fig. 5 Radio spectral variability of NRAO 150

Acknowledgements This research has made use of the Radio Reference Frame Image Database (RRFID) United States Naval Observatory (USNO), and has made use of the data from Radio Astronomy Observatory , University of Michigan, which is supported by the National Natural Science Foundation and the by funds of University of Michigan. The work is supported by Chinese NKBRSF grant G19990754.

References

Bääth L. B., Cotton W. D., Counselman I. I. et al., 1980, A&A, 86, 364
Chu H. S., Bååth L. B., Zhang F. J. et al., 1996, A&A, 307, 15
Kellermann K. I. et al., 1977, ApJ, 211, 658
Kellermann K. I., Jauncey D. L., Cohen M. H. et al., 1971, ApJ, 169, 1
Ma C., Arias E. F., Eubanks T. M. et al., 1998, ApJ, 116, 516
Mutel R. L., Phillips R. B., 1980, ApJ, 241, L73
Phillips R. B., Shaffer D. B., 1983, ApJ, 271, 32
Roellig T. L., Becklin E. E., Impey M. W., 1976, ApJ, 304, 646
Schwab F. R., Cotton W. D., 1983, AJ, 88, 688
Shaffer D. B., Schilizzi R. T., 1975, AJ, 80, 753